

# Thermal Stresses in Functionally Graded Metal-Ceramic Plates

Gutierrez-Miravete, Ernesto<sup>1,\*</sup>

<sup>1</sup>Rensselaer at Hartford

\* 275 Windsor Street, Hartford, CT 06120; gutiee@rpi.edu

**Abstract:** Functionally graded composite materials are attracting interest among design engineers since structural component properties can be designed and customized into finished parts through processing. The controlled variable is the concentration of reinforcing particles at various points within the component. While locally isotropic, part properties can be made to vary in a controlled manner from point to point. This paper described modeling work aimed at the determination of temperature distributions and the associated thermal stresses in functionally graded materials. Material properties are determined from the values of those of the elementary constituents using the rule of mixtures and the Mori-Tanaka method. The thermal stress module in COMSOL is used to calculate the resulting temperature and stress fields for plates subjected to various boundary conditions.

**Keywords:** Functionally-graded materials, metal-ceramic composite, thermal stresses.

## 1. Introduction

Functionally graded, metal-ceramic (FGMC) composites are materials consisting of fine hard particles (reinforcement) dispersed in a ductile matrix (metal) where the spatial distribution of reinforcing particles is carefully controlled so as to optimize the functional thermal and mechanical responses of manufactured components [1], [2]. FGMs are locally isotropic at any given point but the material properties vary with position depending on the relative proportions of matrix and reinforcement. This variation is accomplished through the control of the volume fraction of metal and ceramic constituents. The mechanical and thermo-mechanical responses of FGMs have been the subject of a large amount of research work over the past decade or so [3]-[6]. However, since they are an entirely new type of material, more study of their behavior is needed so that they can be utilized with confidence in applications. This paper describes work carried out at RPI, designed to obtain insight on the

thermomechanical behavior of functionally graded materials by investigating the development of thermal stresses in metal-ceramic composite plates subject to selected thermal and mechanical boundary conditions.

## 2. System Description

The specific system investigated is nickel-zirconia. The system was selected since it is the basis of components widely used in the high temperature propulsion industry. For simplicity, average values of all the material properties in the temperature range considered were used. Table 1 shows the values of all the material properties used in this work.

**Table 1:** Material Properties

Property	Ni	ZrO <sub>2</sub>
$\rho$ (kg/m <sup>3</sup> )	8908	6000
E (Pa)	2e11	2.1e11
$\nu$ (-)	0.31	0.3
k (W/m K)	91	2
$\alpha$ (1/K)	13.4e-6	10.3e-6

The volume fraction of ZrO<sub>2</sub> was assumed to vary only across the thickness of the plate in accordance to the following expression

$$V_2 = V_b + (V_t - V_b) \cdot \left( \frac{1}{2} + \frac{z}{H} \right)^p$$

where  $V_b$  and  $V_t$  are the volume fractions of ZrO<sub>2</sub> at the lower and upper surfaces of the plate, respectively,  $H$  is the plate thickness,  $z$  is the distance measured from the center of the plate and  $p$  is a controllable parameter. The volume fraction of Ni across the thickness was then given by

$$V_1 = 1 - V_2$$

The subscripts 1 and 2 refer to Ni and ZrO<sub>2</sub>, respectively.

The values of density  $\rho$ , thermal conductivity  $k$ , and thermal expansion coefficient  $\alpha$  for points inside the FG plate were calculated from the volume fractions using the rule of mixtures, e.g.

$$\rho_{FGM} = \rho_1 \cdot V_1 + \rho_2 \cdot V_2$$

The values of the mechanical properties were computed using the Mori-Tanaka method [7]. According to this, the bulk modulus of the FG plate is given by

$$K = K_{FGM} = K_1 + \frac{(K_2 - K_1) \cdot V_2}{\left(1 + \frac{(1 - V_2)(K_2 - K_1)}{K_1 + \left(\frac{4}{3}\right)\mu_1}\right)}$$

And the shear modulus for is given by

$$\mu_{FGM} = \mu_1 + \frac{(\mu_2 - \mu_1) \cdot V_2}{\left(1 + \frac{(1 - V_2)(\mu_2 - \mu_1)}{\mu_1 + f_1}\right)}$$

where

$$f_1 = \frac{\mu_1 \cdot (9K_1 + 8\mu_1)}{6 \cdot (K_1 + 2\mu_1)}$$

From the above, Poisson's ration and the elastic modulus are obtained as

$$\nu_{FGM} = \frac{1}{2 \cdot \left(1 + \frac{\mu_{FGM}}{\lambda}\right)}$$

$$E_{FGM} = 3(1 - 2\nu_{FGM})K$$

where

$$\lambda = K - 2\mu_{FGM}/3$$

Plates of various shapes were considered but only results for square plates of dimensions 0.5 by 0.5 m and 0.025 m in thickness are presented in this paper. Temperatures of 293.15 and 493.15 K were applied on the lower and upper surfaces of the plates with the lower value used as reference for thermal strain. Although various mechanical boundary conditions were investigated, only results for plates with all edges clamped and those with one edge clamped and all the other edges free are presented here. Moreover, while values of the power parameter p in the range from 0.1 to 10 were investigated, only results for the case p=10 (mostly metal plate with a layer of ceramic rich material near the upper surface) are presented here.

### 3. Use of COMSOL Multiphysics

The solution of thermal stress problems requires determination of the temperature distribution inside the plate. This is a steady state

heat conduction problem and the governing equation is Laplace's equation. Once the temperature field is known, the equations of linear elasticity must be solved to obtain the displacement field. Finally, differentiation of the displacements and use of Hooke's law yields the thermal stresses.

The Thermal Stress module in COMSOL Multiphysics was used to build the model. A mapped mesh strategy was used to mesh the plate with second order brick elements. Models using a mesh consisting of 10 by 10 elements on the plane with 10 elements through the thickness produced displacement results that varied little upon further refinement.

### 4. Results

The results for the plate clamped all around will be presented first. Figure 1 shows the computed temperature distribution along the thickness of the plate. The ZrO<sub>2</sub>-rich layer near the upper surface of the plate has a thermal barrier coating effect as shown by an increasing value of the slope (which results in lower metal temperatures, a highly desirable situation). Since the temperature is not considered to be affected by the stress field, the same temperature profile was obtained for all the different mechanical boundary conditions.

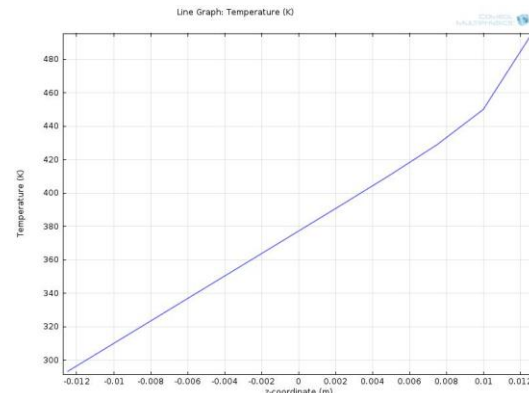


**Figure 1.** Computed temperature versus distance along the thickness of the plate.

Figure 2 shows the computed values of the vertical displacement of the plate. As expected,

the thermal expansion effect makes the plate bend down with the maximum deflection at the center of the plate.

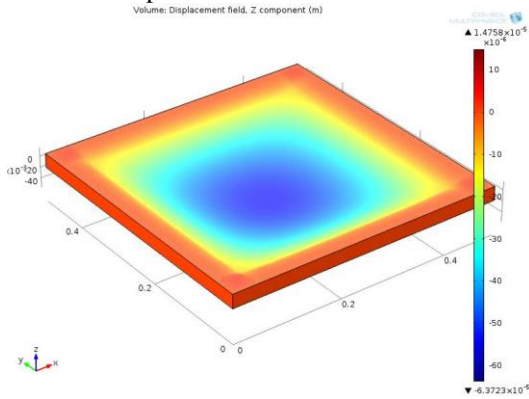


**Figure 2.** Computed vertical displacement. Plate clamped around all edges.

Figure 3 shows the variation of the longitudinal stress component along the plate thickness at one of the corner edges. The stress distribution is tensile in the lower half of the plate and compressive in the upper half and the zero stress point is not in the middle of the plate. Moreover, the enhancing compressive effect of the ceramic rich layer is shown by the change in slope in the curve. In contrast, for the all-metal or all-ceramic plates the stress distribution is linear throughout and the neutral point is at the center of the plate.

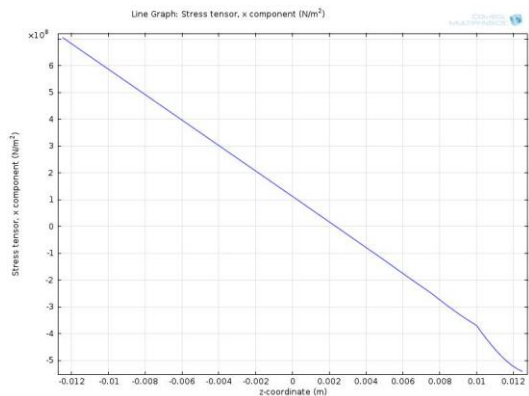


**Figure 3.** Longitudinal stress distribution along the plate thickness. Plate clamped around all edges.

Figure 4 shows the computed vertical displacement for the plate with one edge clamped and all other ends free. As expected, the thermal expansion effect makes the plate bend

down with the maximum deflection at the corners of the free end.

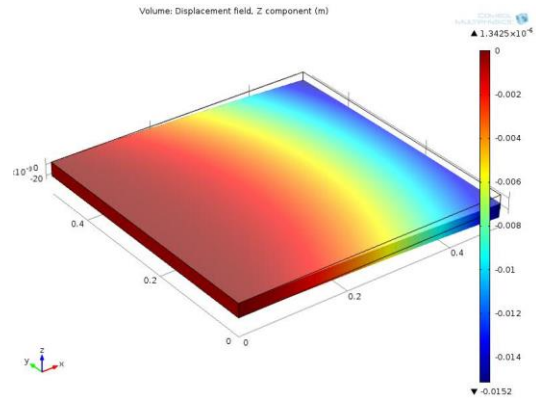


**Figure 4.** Computed vertical displacement. Plate clamped at one edge, all others free.

Figure 5 shows the computed values of the longitudinal stress as a function of thickness along the plate at one of the corners of the free end. The stress distribution is complex and unexpected. The ceramic rich layer at the top of the plate is in a compressive stress state while regions in the plate consisting primarily of metal go from a tensile state near the top of the plate to a state of mild compressive stress on the lower half of the plate. This behavior is in sharp contrast to the one obtained for a pure metal plate (or ceramic) where the thermal stress is compressive on the hot side of the plate and tensile on the cold side. The difference in response must be taken into account when designing FG components.

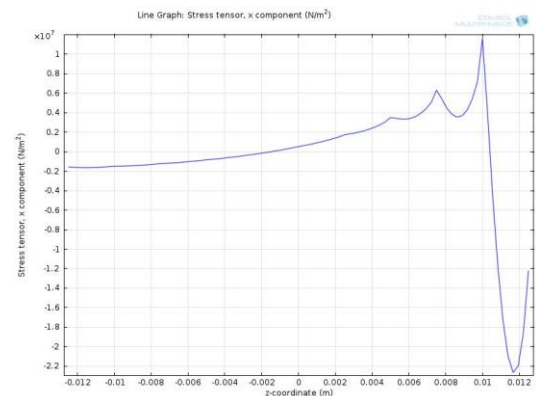


**Figure 5.** Longitudinal stress distribution along the plate thickness. Plate clamped at one edge, all others free.

## 5. Conclusions

COMSOL Multiphysics can be used to develop finite element models that produce reliable predictions of deformation and thermal stresses in functionally graded metal-ceramic composite plates subject to various thermal and mechanical boundary conditions.

## 6. References

1. Chawla, N. and Chawla, K.K. Metal Matrix Composites, 2<sup>nd</sup> ed., Springer, New York, 2013.
2. Mahamood, R.M. et al. Functionally Graded Materials: An Overview, Proceedings of the World Congress in Engineering, London, U.K. July 4-6, 2012, **Vol III**, pp. 1593-1597, 2012.
3. Birman, V. and Byrd, L.W. Modeling and Analysis of Functionally Graded Materials and Structures, Applied Mechanics Reviews, ASME, **60**, pp. 195-216 (September 2007).
4. Kim, J. and Reddy, J.N. Analytical solutions for bending, vibration and buckling of FGM plates using a couple stress-based third-order theory, Composite Structures, **103**, pp. 86-98, (2013).
5. Sankar, B.V. and Tzeng, J.T. Thermal Stresses in Functionally Graded Beams, AIAA Journal, **40** (6) pp. 1228-1232 (June 2002)
6. Matsunaga, H. Stress analysis of functionally graded plates subjected to thermal and mechanical loadings, Composite Structures, **87**, pp. 344-357 (2009).